

# Geometric Measure of Quantum Discord for Entanglement of Total Dirac Fields in Noninertial Frames

Wen-Chao Qiang<sup>1</sup> · Lei Zhang<sup>2</sup>

Received: 1 October 2016 / Accepted: 7 December 2016 / Published online: 19 December 2016  
© Springer Science+Business Media New York 2016

**Abstract** We study the geometric measure of quantum discord of total Dirac fields in non-inertial frames. As a comparison, we also calculate the corresponding geometric measure of entanglement of the same system. We discuss the properties of geometric measure of quantum discord and geometric measure of entanglement for this system with acceleration parameter and the parameter describing the entangle degree of the system in detail. Our results show that from an overall perspective, two geometric measures have similar behavior with the variation of the entangle parameter and the acceleration parameter. We find that this tripartite system is monogamous for the geometric measure of quantum discord.

**Keywords** Quantum discord · Entanglement of total Dirac fields · Geometric measure

## 1 Introduction

In our last paper, we briefly reviewed the research on entanglements shared by inertial and noninertial observers. We concentrated our attention to studying the entanglements of Dirac fields in a noninertial frame and mainly investigated three bipartite subsystems of this tripartite system [1]. The analytical expressions of geometric discord and geometric measure of entanglement both for every two-qubit system were presented. The behaviors of two geometric measurements, which we obtained, were discussed in detail and compared with each other. We also reported some partial conservative relations for concurrence, mutual

---

✉ Wen-Chao Qiang  
qwcqj@163.com

<sup>1</sup> Faculty of Science, Xi'an University of Architecture and Technology, Xi'an, 710055, China

<sup>2</sup> Huaqing College, Xi'an University of Architecture and Technology, Xi'an, 710055, China

information, geometric discord and geometric measure of entanglement. Researchers who interested in this subject can refer to Ref. [1] and references therein.

Above work has deepened our understanding of the Dirac fields from the respect of geometric discord, but it is not complete. We know nothing about the correlation properties of the whole system. However, the correlation properties of the total system are very important. Alsing et al. investigated the maximally entangled initial state shared by two observers, one of which moves with a uniform acceleration. They calculated the entanglement of formation, the logarithmic negativity and the mutual information for three bipartite subsystems and the residual tangle (or three tangle) for whole tripartite system [2]. Hwang et al. investigated the tripartite entanglement of Greeberger-Horne-Zeilinger (GHZ) state and W state in a noninertial frame using  $\pi$ -tangle [3]. Wang et al. also studied a GHZ state initially shared by three persons. They assumed one or two persons stay stationary while other two or one persons move with uniform accelerations. They calculated all  $\pi$ -tangles for bipartite subsystems and the tripartite system [4]. Alsing and Wang obtained contradictory results on whether entanglements exist only in bipartite systems or tripartite systems. Perhaps the different results come from the factor that they use different measures. To further understand this problem, we attempt to study this issue from another aspect. We shall use geometric discord and geometric measure of the entanglement to investigate the whole Dirac fields in a noninertial frame.

This paper is arranged as follows. In the next section, we present a short review of geometric measure of quantum discord and geometric measure of entanglement both from another respect. In Section 3 we derive the analytic expressions of geometric discord for total Dirac's fields in a noninertial frame. Section 4 devotes to calculate the geometric measure of the entanglement for the same system. Discussions and summary are provided in Section 5.

## 2 A Further Brief Review of Geometric Discord and Geometric Measure of Entanglement from Another Perspective

We have briefly reviewed geometric discord and geometric measure of entanglement in Ref. [1], but did not mention some details that will be used in this paper. Readers interested in these two kinds of geometric measures had better refer to our early paper and references therein. Here, we replenish some formulas used to calculate geometric discord and geometric measure of entanglement.

Since Dakić et al. obtained a formula to calculate geometric discord for two-qubit state [5], Luo and Fu extended Dakić's result to general bipartite states [6], Rana and Hassan derived a rigorous lower bound to the geometric discord for any bipartite state, respectively, which is exact for a  $2 \times d$  system (with a measurement on the qubit) [7, 8]. On the other hand, Tufarelli proposed another formula to calculate geometric discord for a  $2 \times d$  system that is applicable to  $d \rightarrow \infty$  case [9],

$$D_G(\rho_{AB}) = \text{tr}(S) - \lambda_{\max}(S), \quad (1)$$

where  $S = \text{tr}[\mathbf{v}\mathbf{v}^t]$ ,  $\mathbf{v} = \text{tr}_A[\rho_{AB}\sigma]$ ,  $\sigma$  are the Pauli matrices and  $\mathbf{v}^t$  stands for the transpose of  $\mathbf{v}$ . It is worth noting, first, in order to normalize the maximum value of the geometric discord for Bell state to 1, Tufarelli added a factor 2 to the original definition. In this paper, we shall use (1) to calculate the geometric discord, but to consist with our early work, the results will be divided by 2; second, it is obvious, (1) can be extended to any system that contains one qubit, on which a measurement makes. For example, for state  $\rho_{ABC}$  with

subsystem  $A$  is a qubit, the definition  $\mathbf{v}$  may remain unchanged, but  $S$  can be modified as  $S = \text{tr}_{BC}[\mathbf{v}\mathbf{v}^t]$ . This extension will be illustrated in the next section.

As for the geometric measure of a entanglement, based on the theorem stating that any reduced  $(n - 1)$ -qubit state uniquely determines the geometric measure of the original  $n$ -qubit pure state [10], for any three-qubit stats  $\rho_{ABC}$ , Tamaryan et al. first rewrote the square of the entanglement eigenvalues as

$$\Lambda_{\max}^2 = \max_{\rho_1 \rho_2 \rho_3} \text{tr}(\rho_{ABC} \rho_1 \otimes \rho_2 \otimes \rho_3) \tag{2}$$

$$= \max_{\rho_1 \rho_2} \text{tr}(\rho_{ABC} \rho_1 \otimes \rho_2). \tag{3}$$

Then, they derived the following expression [11]

$$\Lambda_{\max}^2 = \frac{1}{4} \max_{s_1^2=s_2^2=1} (1 + \mathbf{s}_1 \cdot \mathbf{r}_\mu + \mathbf{s}_2 \cdot \mathbf{r}_\nu + g_{ij} s_{1i} s_{2j}),$$

$$\{\mu, \nu\} = \{A, B\}, \{B, C\}, \{A, C\}. \tag{4}$$

where  $\mathbf{s}_1$  and  $\mathbf{s}_2$  are two unit Bloch vectors of the density matrices of the single-qubit  $\rho_1$  and  $\rho_2$  states respectively, which will be determined and

$$\begin{aligned} \mathbf{r}_\mu &= \text{tr}(\rho_\mu \boldsymbol{\sigma}) \\ \mathbf{r}_\nu &= \text{tr}(\rho_\nu \boldsymbol{\sigma}) \\ g_{ij} &= \text{tr}(\rho_{\mu\nu} \sigma_i \otimes \sigma_j). \end{aligned} \tag{5}$$

They finally gave an analytical expression of  $\mathbf{s}_1$  and  $\mathbf{s}_2$  under some condition, which we shall not use. In the Section 4, we are going to optimize (4) directly for our problem.

### 3 Geometric Discord for Total Dirac Fields in Noninertial Frames

In our early paper [1], we have assumed that Alice and Rob share initially the entangled state in an inertial frame,

$$|\psi\rangle_{AR} = \alpha|0_A 0_R\rangle + \sqrt{1 - \alpha^2}|1_A 1_R\rangle. \tag{6}$$

We first derive the geometric discord of the total system in the initial state, that is in an inertial frame. The density operator can be calculated using (6),

$$\begin{aligned} \rho_0 &= \alpha^2|0_A 0_R\rangle\langle 0_R 0_A| + (1 - \alpha^2)|1_A 1_R\rangle\langle 1_R 1_A| \\ &+ \alpha\sqrt{1 - \alpha^2}(|1_A 1_R\rangle\langle 0_R 0_A| + |0_A 0_R\rangle\langle 1_R 1_A|). \end{aligned} \tag{7}$$

Though generally speaking, the geometric discord is not symmetrical for every subsystem of the system, but we noticed that (6) and (7) are symmetrical for Alice and Rob. Therefore, doing von Neumann measurements on Alice’s or Rob’s qubit will give the same results. For example, if we do this measurement on Alice’s qubit, we find

$$\begin{aligned} \mathbf{v} &= \{\alpha\sqrt{1 - \alpha^2}(|1_R\rangle\langle 0_R| + |0_R\rangle\langle 1_R|), \\ &i\alpha\sqrt{1 - \alpha^2}(|0_R\rangle\langle 1_R| - |1_R\rangle\langle 0_R|), \\ &\alpha^2|0_R\rangle\langle 0_R| - (1 - \alpha^2)|1_R\rangle\langle 1_R|\}. \end{aligned} \tag{8}$$

$$S = \begin{pmatrix} 2\alpha^2(1 - \alpha^2) & 0 & 0 \\ 0 & 2\alpha^2(1 - \alpha^2) & 0 \\ 0 & 0 & 1 - 2\alpha^2 + 2\alpha^4 \end{pmatrix}. \tag{9}$$

Matrix  $S$  has tree eigenvalues  $\{2\alpha^2(1 - \alpha^2), 2\alpha^2(1 - \alpha^2), 1 - 2\alpha^2 + 2\alpha^4\}$  and  $1 - 2\alpha^2 + 2\alpha^4 \geq 2\alpha^2(1 - \alpha^2)$ . We finally obtain

$$D_G(\rho_0) = 2\alpha^2(1 - \alpha^2). \tag{10}$$

After sharing his own qubit, Rob moves with respect to Alice with a uniform acceleration  $a$ . Using the single-mode approximation, Rob’s vacuum and one-particle states  $|0_R\rangle$  and  $|1_R\rangle$  in Minkowski space are transformed into [2]

$$\begin{aligned} |0_R\rangle &\rightarrow \cos r|0_I 0_{II}\rangle + \sin r|1_I 1_{II}\rangle, \\ |1_R\rangle &\rightarrow |1_I 0_{II}\rangle, \end{aligned} \tag{11}$$

where  $r$  is the acceleration parameter, which is in the range  $0 \leq r \leq \pi/4$  for  $0 \leq a \leq \infty$ ,  $|n_I\rangle$  and  $|n_{II}\rangle$  ( $n = 0, 1$ ) are the mode decomposition in the two causally disconnected regions in Rindler space. Using (11), we obtain

$$\begin{aligned} |\psi\rangle_{A III} &= \alpha|0_A\rangle \otimes (\cos r|0_I 0_{II}\rangle + \sin r|1_I 1_{II}\rangle) \\ &\quad + \sqrt{1 - \alpha^2}|1_A 1_I 0_{II}\rangle, \end{aligned} \tag{12}$$

and corresponding density operator

$$\begin{aligned} \rho_{AIII} &= \alpha^2 \cos^2 r |0_A 0_I 0_{II}\rangle \langle 0_{II} 0_I 0_A| + \alpha^2 \sin^2 r |0_A 1_I 1_{II}\rangle \langle 1_{II} 1_I 0_A| \\ &\quad + \alpha \sqrt{1 - \alpha^2} [(\cos r |0_A 0_I 0_{II}\rangle + \sin r |0_A 1_I 1_{II}\rangle) \langle 0_{II} 1_I 1_A| \\ &\quad \quad + |1_A 1_I 0_{II}\rangle (\cos r \langle 0_{II} 0_I 0_A| + \sin r \langle 1_{II} 1_I 0_A|)] \\ &\quad + \alpha^2 \cos r \sin r (|0_A 1_I 1_{II}\rangle \langle 0_{II} 0_I 0_A| + |0_A 0_I 0_{II}\rangle \langle 1_{II} 1_I 0_A|) \\ &\quad + (1 - \alpha^2) |1_A 1_I 0_{II}\rangle \langle 1_A 1_I 0_{II}|. \end{aligned} \tag{13}$$

If we do von Neumann measurements on Alice’s qubit in  $\rho_{AIII}$ , we would obtain the same results as (10). In order to test the influence of the Unruh effect [12, 13] on geometric discord, we must measure the qubit in model  $I$ . We can calculate vector  $\mathbf{v}$  and matrix  $S$  according to above equation, respectively, as follows,

$$\begin{aligned} \mathbf{v} &= \{\alpha \sqrt{1 - \alpha^2} \cos(r) (|1_A 0_{II}\rangle \langle 0_{II} 0_A| + |0_A 0_{II}\rangle \langle 0_{II} 1_A|) \\ &\quad + \alpha^2 \sin(r) \cos(r) (|0_A 1_{II}\rangle \langle 0_{II} 0_A| + |0_A 0_{II}\rangle \langle 1_{II} 0_A|), \\ &\quad i[\alpha \sqrt{1 - \alpha^2} \cos(r) (|0_A 0_{II}\rangle \langle 0_{II} 1_A| - |1_A 0_{II}\rangle \langle 0_{II} 0_A|) \\ &\quad + \alpha^2 \sin(r) \cos(r) (|0_A 0_{II}\rangle \langle 1_{II} 0_A| - |0_A 1_{II}\rangle \langle 0_{II} 0_A|)], \\ &\quad \alpha^2 \cos^2(r) |0_A 0_{II}\rangle \langle 0_{II} 0_A| - \alpha^2 \sin^2(r) |0_A 1_{II}\rangle \langle 1_{II} 0_A| \\ &\quad - (1 - \alpha^2) |1_A 0_{II}\rangle \langle 0_{II} 1_A| \\ &\quad - \alpha \sqrt{1 - \alpha^2} \sin(r) (|0_A 1_{II}\rangle \langle 0_{II} 1_A| + |1_A 0_{II}\rangle \langle 1_{II} 0_A|)\} \end{aligned} \tag{14}$$

$$s = \begin{pmatrix} 2\alpha^2 \cos^2(r) [1 - \alpha^2 \cos^2(r)] & 0 & 0 \\ 0 & 2\alpha^2 \cos^2(r) [1 - \alpha^2 \cos^2(r)] & 0 \\ 0 & 0 & \frac{1}{2} [(1 - 2\alpha^2 \cos^2(r))^2 + 1] \end{pmatrix} \tag{15}$$

Because

$$\begin{aligned} &\frac{1}{2} \left[ (1 - 2\alpha^2 \cos^2(r))^2 + 1 \right] - 2\alpha^2 \cos^2(r) [1 - \alpha^2 \cos^2(r)] \\ &= (1 - 2\alpha^2 \cos^2(r))^2 \geq 0, \end{aligned} \tag{16}$$

the maximum value of the eigenvalues of  $S$  is

$$\lambda_{\max} = \frac{1}{2} \left[ \left( 1 - 2\alpha^2 \cos^2(r) \right)^2 + 1 \right]. \tag{17}$$

We finally obtain

$$D_G(\rho_{AIII}) = 2\alpha^2 \cos^2(r) \left[ 1 - \alpha^2 \cos^2(r) \right]. \tag{18}$$

We notice when  $r = 0$ , (18) is reduced to (10). We plot  $D_G(\rho_{AIII})$  as functions of  $\alpha$  and  $r$  in Fig. 1.

Getting geometric discord of the state  $\rho_{AIII}$  enables us to study the monogamy of this state. The monogamy is an important property of a tripartite system. A correlation measure  $\mathcal{Q}$  is monogamous if and only if the following Coffman-Kundu-Wootters (CKW) monogamy inequality

$$\mathcal{Q}_{A|BC} \geq \mathcal{Q}_{AB} + \mathcal{Q}_{AC} \tag{19}$$

holds for any tripartite state  $\rho_{ABC}$  [14]. Recalling we have calculated in Ref.[1]

$$D_{G(I|II)} = D_G(\rho_{III}) = \begin{cases} 2\alpha^4 \sin^2(r) \cos^2(r), \\ \alpha^2 [5\alpha^2 - 2(1 - \alpha^2) \cos(2r) + \alpha^2 \cos(4r) - 6] + 2 \geq 0; \\ \frac{1}{2} [3\alpha^4 - 3\alpha^2 - (1 - \alpha^2) \alpha^2 \cos(2r) + 1], \\ \text{otherwise.} \end{cases} \tag{20}$$

we now need to get  $D_{G(I|A)}$ . Using (1) or procedures used to calculate  $D_G(\rho_{III})$  in Ref. [1], we obtain

$$D_{G(I|A)} = \begin{cases} 2\alpha^2 (1 - \alpha^2) \cos^2(r), \\ \alpha^2 [5\alpha^2 - 2(1 - \alpha^2) \cos(2r) + \alpha^2 \cos(4r) - 6] + 2 \geq 0; \\ \frac{1}{2} [1 - \alpha^2 [2 \sin^2(r) + \alpha^2 \cos(2r)(1 - \cos(2r))]], \\ \text{otherwise.} \end{cases} \tag{21}$$

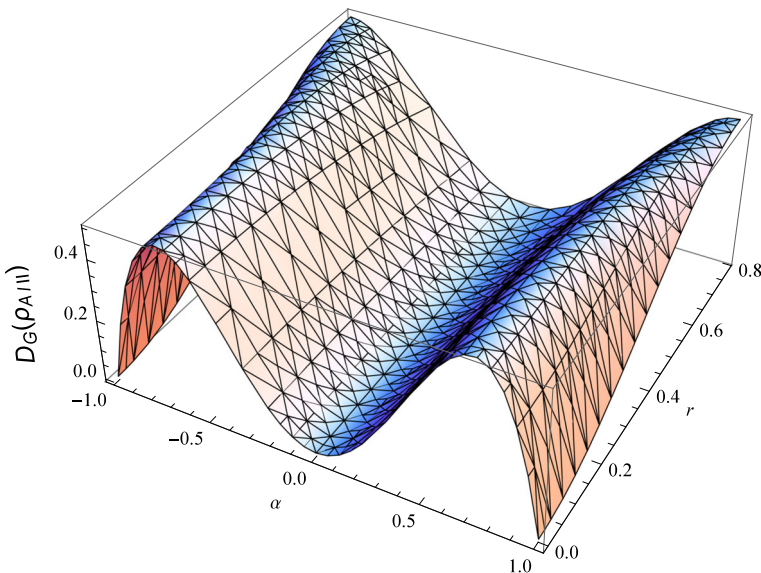


**Fig. 1** (Color online) Plots of geometric measure of quantum discord  $D_G(\rho_{AIII})$  as functions of  $\alpha$  and  $r$

Using (18), (21) and (20) and doing some simplification, we finally obtain

$$\begin{aligned}
 & D_{G(I|AII)} - D_{G(I|A)} - D_{G(I|II)} \tag{22} \\
 = & \begin{cases} 0, & 2 - \alpha^2 [6 - 5\alpha^2 - \alpha^2 \cos(4r) + 2(1 - \alpha^2) \cos(2r)] \geq 0; \\ -\frac{1}{2} [2 - \alpha^2 [6 - 5\alpha^2 - \alpha^2 \cos(4r) + 2(1 - \alpha^2) \cos(2r)]] > 0, & \text{otherwise.} \end{cases}
 \end{aligned}$$

(22) shows the inequality  $D_{G(I|AII)} \geq D_{G(I|A)} + D_{G(I|II)} \geq 0$  holds in the present situation. On the other hand, as we have pointed out if we do geometric measurements of quantum discord on Alice’s qubit, we would obtain  $D_{G(A|III)} = D_G(\rho_0)$  as (10). In addition, from Ref. [1] we know,

$$D_{G(A|I)} = D_G(\rho_{AI}) = \begin{cases} 2\alpha^2 (1 - \alpha^2) \cos^2(r), \\ 4 + \alpha^4 [15 + \cos(4r)] \geq 16\alpha^2; \\ \frac{1}{8} \{4 + \alpha^4 [7 + \cos(4r)] - 8\alpha^2 [1 - (1 - \alpha^2) \cos(2r)]\}, \\ \text{otherwise.} \end{cases} \tag{23}$$

$$D_{G(A|II)} = D_G(\rho_{AII}) = \begin{cases} 2\alpha^2 (1 - \alpha^2) \cos^2(r), \\ 4 + \alpha^4 [15 + \cos(4r)] \geq 16\alpha^2; \\ \frac{1}{8} \{4 + \alpha^4 [7 + \cos(4r)] - 8\alpha^2 [1 + (1 - \alpha^2) \cos(2r)]\}, \\ \text{otherwise.} \end{cases} \tag{24}$$

Substituting (10), (23) and (24) into (19) gives

$$D_{G(A|III)} - D_{G(A|I)} - D_{G(A|II)} = \begin{cases} 0, \\ 4 + \alpha^4 [15 + \cos(4r)] \geq 16\alpha^2; \\ 4\alpha^2 - \frac{1}{4} \{4 + \alpha^4 [15 + \cos(4r)]\} \geq 0, \\ \text{otherwise.} \end{cases} \tag{25}$$

Above equation shows that geometric measurements of quantum discord on Alice’s qubit also satisfy CKW monogamy inequality. Combining (22) and (25), we conclude that the system  $\rho_{AIII}$  is monogamous for the geometric discord.

### 4 Geometric Measure for Total Dirac Fields in Noninertial Frames

We first calculate the geometric measure of the initial state  $|\psi\rangle_{AR}$ . According to (7), we can easily obtain the density matrix of the initial state  $|\psi\rangle_{AR}$ .

$$\rho_0 = \rho_{AR} = \begin{pmatrix} \alpha^2 & 0 & 0 & \alpha\sqrt{1 - \alpha^2} \\ 0 & 0 & 0 & 0 \\ 0 & 0 & 0 & 0 \\ \alpha\sqrt{1 - \alpha^2} & 0 & 0 & 1 - \alpha^2 \end{pmatrix}, \tag{26}$$

which is an X state. Its concurrence can be easily obtained  $C_0 = 2\alpha\sqrt{1 - \alpha^2}$ . Substituting it into (9) of Ref. [1], we obtain

$$E_g(|\psi\rangle_{AR}) = \max(\alpha^2, 1 - \alpha^2). \tag{27}$$

We now calculate the geometric measure of the total system. We have derived  $\mathbf{r}_\mu, \mathbf{r}_\nu$  and matrix  $g$  for  $\rho_{AI}, \rho_{AII}$  and  $\rho_{III}$ , and list the results in Table 1.

Generally speaking, we can use any one of  $\rho_{AI}, \rho_{AII}$  and  $\rho_{III}$  to calculate the geometric measure of entanglement of the total system. Here, in order to get an intuitive perception,

**Table 1** A list of  $\rho_{\mu\nu}$ ,  $\mathbf{F}_\mu$ ,  $\mathbf{F}_\nu$  ( $\{\mu, \nu\} = \{A, I\}, \{A, II\}, \{I, II\}$ ) and corresponding matrices  $g$

	$\rho_{\mu\nu}$	$\mathbf{F}_\mu$ $\mathbf{F}_\nu$	$g$
$\rho_{AI}$	$\begin{pmatrix} \alpha^2 \cos^2(r) & 0 & 0 & \alpha\sqrt{1-\alpha^2} \cos(r) \\ 0 & \alpha^2 \sin^2(r) & 0 & 0 \\ 0 & 0 & 0 & 0 \\ \alpha\sqrt{1-\alpha^2} \cos(r) & 0 & 0 & 1-\alpha^2 \end{pmatrix}$	$\{0, 0, 2\alpha^2 - 1\}$ $\{0, 0, 2\alpha^2 \cos^2(r) - 1\}$	$\begin{pmatrix} 2\alpha\sqrt{1-\alpha^2} \cos(r) & 0 & 0 \\ 0 & -2\alpha\sqrt{1-\alpha^2} \cos(r) & 0 \\ 0 & 0 & 1-2\alpha^2 \sin^2(r) \end{pmatrix}$
$\rho_{AII}$	$\begin{pmatrix} \alpha^2 \cos^2(r) & 0 & 0 & \alpha^2 \cos(r) \sin(r) \\ 0 & 0 & 0 & 0 \\ 0 & 0 & 0 & 0 \\ 0 & 0 & 1-\alpha^2 & 0 \\ \alpha^2 \cos(r) \sin(r) & 0 & 0 & \alpha^2 \sin^2(r) \end{pmatrix}$	$\{0, 0, 2\alpha^2 - 1\}$ $\{0, 0, 1 - 2\alpha^2 \sin^2(r)\}$	$\begin{pmatrix} 2\alpha\sqrt{1-\alpha^2} \sin(r) & 0 & 0 \\ 0 & 2\alpha\sqrt{1-\alpha^2} \sin(r) & 0 \\ 0 & 0 & 2\alpha^2 \cos^2(r) - 1 \end{pmatrix}$
$\rho_{III}$	$\begin{pmatrix} \alpha^2 \cos^2(r) & 0 & 0 \\ 0 & \alpha^2 \sin^2(r) & \alpha\sqrt{1-\alpha^2} \sin(r) \\ 0 & \alpha\sqrt{1-\alpha^2} \sin(r) & 1-\alpha^2 \\ 0 & 0 & 0 & 0 \end{pmatrix}$	$\{0, 0, 2\alpha^2 \cos^2(r) - 1\}$ $\{0, 0, 1 - 2\alpha^2 \sin^2(r)\}$	$\begin{pmatrix} \alpha^2 \sin(2r) & 0 & 0 \\ 0 & -\alpha^2 \sin(2r) & 0 \\ 0 & 0 & 2\alpha^2 - 1 \end{pmatrix}$

we first numerically optimize  $4\Lambda^2 = 1 + \mathbf{s}_1 \cdot \mathbf{r}_\mu + \mathbf{s}_2 \cdot \mathbf{r}_\nu + g_{ij}s_1s_2j$  for  $\rho_{A_I}$ . For this end, we let

$$\begin{aligned} \mathbf{s}_1 &= \{\sin(\theta_1) \cos(\phi_1), \sin(\theta_1) \sin(\phi_1), \cos(\theta_1)\}, \\ \mathbf{s}_2 &= \{\sin(\theta_2) \cos(\phi_2), \sin(\theta_2) \sin(\phi_2), \cos(\theta_2)\}, \end{aligned} \tag{28}$$

and obtain

$$\begin{aligned} 4\Lambda^2 &= (\cos(\theta_A) - 1)(\cos(\theta_1) - 1) \\ &\quad + 2\alpha\sqrt{1 - \alpha^2} \cos(r) \sin(\theta_1) \sin(\theta_A) \cos(\phi_{A1}) \\ &\quad + 2\alpha^2 \left( \cos(\theta_A) + \cos(\theta_1) \left( \cos^2(r) - \cos(\theta_A) \sin^2(r) \right) \right), \end{aligned} \tag{29}$$

where  $\phi_{A1} = \phi_A + \phi_1$ . We can now maximize  $4\Lambda^2$  for a given set of  $\{\alpha, r\}$  and obtain  $E_g = 1 - \Lambda_{\max}^2$  numerically. We visualize our result  $E_g$  in Fig. 2. In fact, we have also maximized  $4\Lambda^2$  for a given set of  $\{\alpha, r\}$  according to  $\rho_{A_{III}}$  and  $\rho_{I_{III}}$ , respectively. The corresponding plots of  $E_g = 1 - \Lambda_{\max}^2$  are exactly the same as Fig. 2.

Next, we work out the analytic expression of  $E_g(\rho_{A_{III}})$ . Because  $0 \leq \alpha^2 \leq 1$  and  $0 \leq r \leq \pi/4$ ,  $\min(r_{III3}) = 1 - 2\alpha^2 \sin(\pi/4)^2 \geq 1 - \alpha^2 \geq 0$ ,  $r_{III3} = 1 - 2\alpha^2 \sin(\pi/4)^2 \geq 0$ . Further more, since  $r_{A3} - g_{33} = 2\alpha^2 \sin(\alpha)^2 \geq 0$ , therefore, if  $g_{33} \geq 0$ , then  $r_{A3} \geq 0$ ; if  $r_{A3} \leq 0$ , then  $-g_{33} \geq 0$ . In the following, for simplicity, we let  $\omega = g_{11} = g_{22} = 2\alpha\sqrt{1 - \alpha^2} \sin(r)$  and  $r_3 = -g_{33} = 1 - 2\alpha^2 \cos(r)^2$ . Then, there are only three cases need to be considered: (1)  $r_{A3}$ ,  $r_{III3}$  and  $r_3$  are all not negative; (2) only  $r_{A3} \leq 0$ ; (3) only  $r_3 \leq 0$ . We noticed that  $\rho_{A_{III}}$  is similar to W-TYPE state in Ref. [11]. Hence, any vector along  $z$  axis is an eigenvector with eigenvalue  $-r_3$ ; any vector perpendicular to  $z$  axis is an eigenvector with eigenvalue  $\omega$ . These let us denote  $s_1$  and  $s_2$  as:

$$\begin{aligned} \mathbf{s}_1 &= \sin(\theta_1)\mathbf{m} + \cos(\theta_1)\mathbf{n}, \\ \mathbf{s}_2 &= \sin(\theta_2)\mathbf{m} + \cos(\theta_2)\mathbf{n}. \end{aligned} \tag{30}$$

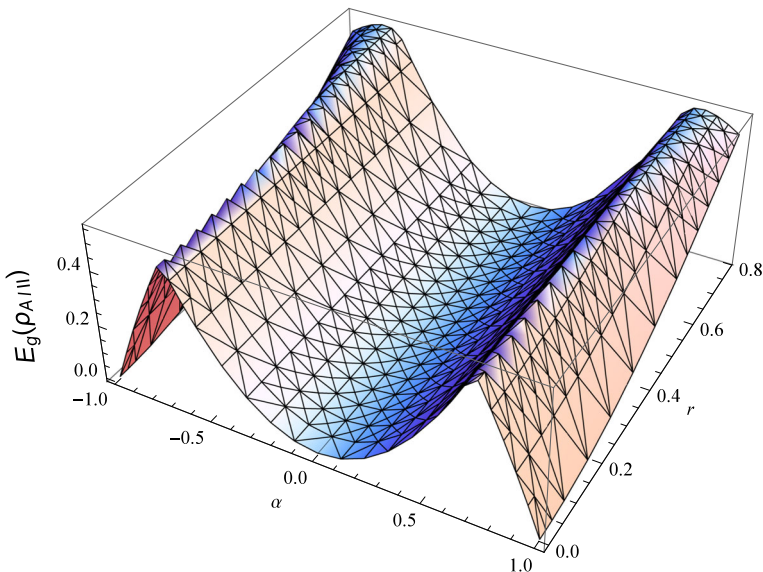


Fig. 2 (Color online) Plots of geometric measure of  $E_g(\rho_{A_{III}})$  as functions of  $\alpha$  and  $r$



where unit vectors  $\mathbf{n}$  and  $\mathbf{m}$  are along with and perpendicular to  $z$  direction, respectively. Substituting  $\mathbf{r}_A, \mathbf{r}_{II}, \mathbf{s}_1, \mathbf{s}_2$ , and  $g$  into  $4\Lambda^2 = 1 + \mathbf{s}_1 \cdot \mathbf{r}_\mu + \mathbf{s}_2 \cdot \mathbf{r}_\nu + g_{ij}s_{1i}s_{2j}$ , we obtain

$$4\Lambda^2 = f(\theta_1, \theta_2) = 1 + r_{A3} \cos(\theta_1) + r_{II3} \cos(\theta_2) + \omega \sin(\theta_1) \sin(\theta_2) - r_3 \cos(\theta_1) \cos(\theta_2). \tag{31}$$

Solving equations

$$\frac{\partial f(\theta_1, \theta_2)}{\partial \theta_1} = 0, \tag{32a}$$

$$\frac{\partial f(\theta_1, \theta_2)}{\partial \theta_2} = 0, \tag{32b}$$

$$\sin(\theta_1)^2 + \cos(\theta_1)^2 = 1, \tag{32c}$$

$$\sin(\theta_2)^2 + \cos(\theta_2)^2 = 1. \tag{32d}$$

for  $\sin(\theta_1), \cos(\theta_1), \sin(\theta_2), \cos(\theta_2)$ , we obtain eight group formulas of  $\sin(\theta_1), \cos(\theta_1), \sin(\theta_2), \cos(\theta_2)$ . Substituting them into  $f(\theta_1, \theta_2)$ , we get six distinct formulas of  $4\Lambda^2$ , the first and third of which are  $\{1 - r_{II3} - r_3 - r_{A3}, 1 - r_{II3} + r_3 + r_{A3}\}$  that do not give the maximum of  $4\Lambda^2$  because  $r_{II3} \geq 0$ . Therefore, there are only four formulas, which may give the maximum of  $4\Lambda^2$ .

$$1 + r_{II3} + r_3 - r_{A3}, \tag{33a}$$

$$1 + r_{II3} - r_3 + r_{A3}, \tag{33b}$$

$$1 + \frac{\text{sgn}(r_{A3}r_{II3}r_3) (R + |r_{A3}r_{II3}r_3|)}{r_3^2 - \omega^2}, \tag{33c}$$

$$1 - \frac{\text{sgn}(r_{A3}r_{II3}r_3) (R - |r_{A3}r_{II3}r_3|)}{r_3^2 - \omega^2}, \tag{33d}$$

with

$$R = |\omega| \sqrt{(r_{II3}^2 - r_3^2 + \omega^2) (r_{A3}^2 - r_3^2 + \omega^2)}. \tag{34}$$

From (33c, 33d) we can see

$$4\Lambda_{max}^2 = \begin{cases} 1 + \frac{R + |r_{A3}r_{II3}r_3|}{r_3^2 - \omega^2}, & r_3^2 - \omega^2 \geq 0 \wedge r_{A3} \geq 0 \wedge r_3 \geq 0; \\ 1 - \frac{R - |r_{A3}r_{II3}r_3|}{r_3^2 - \omega^2}, & r_3^2 - \omega^2 < 0 \wedge r_{A3} \geq 0 \wedge r_3 \geq 0. \end{cases} \tag{35}$$

On the other hand,

$$4\Lambda_{max}^2 = \begin{cases} \max[1 + |r_{A3}| + r_{II3} + |r_3|, 1 + \frac{R - |r_{A3}r_{II3}r_3|}{r_3^2 - \omega^2}], & r_3^2 - \omega^2 \geq 0 \wedge (r_{A3} \leq 0 \vee r_3 \leq 0); \\ \max[1 + |r_{A3}| + r_{II3} + |r_3|, 1 - \frac{R + |r_{A3}r_{II3}r_3|}{r_3^2 - \omega^2}], & r_3^2 - \omega^2 < 0 \wedge (r_{A3} \leq 0 \vee r_3 \leq 0). \end{cases} \tag{36}$$

Substituting  $r_{A3}, r_{II3}, r_3$  and  $\omega$  into (35, 36), we finally obtain

$$4\Lambda_{max}^2 = \begin{cases} 0, r_3^2 - \omega^2 \geq 0 \wedge r_{A3} \geq 0 \wedge r_3 \geq 0; \\ \frac{8\alpha^4(\alpha^2-1)\sin^2(2r)}{7\alpha^4-8\alpha^2+\alpha^4\cos(4r)+2}, \\ r_3^2 - \omega^2 \leq 0 \wedge r_{A3} \geq 0 \wedge r_3 \geq 0; \\ \max[\frac{8\alpha^4(\alpha^2-1)\sin^2(2r)}{7\alpha^4-8\alpha^2+\alpha^4\cos(4r)+2}, \\ 4(1-\alpha^2), 4\alpha^2\cos^2(r)], \\ r_3^2 - \omega^2 \geq 0 \wedge (r_{A3} \leq 0 \vee r_3 \leq 0); \\ \max[0, 4(1-\alpha^2), 4\alpha^2\cos^2(r)], \\ r_3^2 - \omega^2 \leq 0 \wedge (r_{A3} \leq 0 \vee r_3 \leq 0); \end{cases} \tag{37}$$

The plot of  $E_g = 1 - \Lambda_{max}^2$  according to (37) is the same as Fig. 2. For initial state,  $r = 0$ , (37) gives  $E_g = 1 - \Lambda_{max}^2 = \max(1 - \alpha^2, \alpha^2)$ , which coincides with (27).

### 5 Discussion and Summary

We have analytically worked out the geometric discord  $D_G$  and geometric measure of entanglement  $E_g$  for total Dirac fields in the noninertial frames. We now give three useful remarks.

First, Though  $D_G$  and  $E_g$  are not equal, Figs. 1 and 2 shows that from an overall perspective, they have similar behavior with the variation of entangle parameter  $\alpha$  and acceleration parameter  $r$ . From (18) and (37), we see that  $D_G$  and  $E_g$  are symmetry about  $\alpha = 0$ . Recall  $0 \leq r \leq \pi/4$  and  $0 \leq \alpha^2 \leq 1$  as well as  $\partial D_G(\alpha, r)/\partial r = 2\alpha^2 \sin(2r) (2\alpha^2 \cos^2(r) - 1)$ , we see for a given entangle parameter  $\alpha$ ,  $D_G$  increases with the increase of the acceleration parameter  $r$  when  $\cos(r) > \frac{1}{\sqrt{2|\alpha|}}$ ; otherwise, it decrease with the increase of the acceleration parameter  $r$ ; Similarly, because  $\partial D_G(\alpha, r)/\partial \alpha^2 = 2 \cos^2(r)[1 - 2\alpha^2 \cos^2(r)]$ , we know for a given acceleration parameter  $r$ ,  $D_G$  increases with the increase of  $\alpha^2$  when  $\alpha^2 < \frac{1}{2 \cos^2(r)}$ ; otherwise, it decrease with the increase of  $\alpha^2$ ;  $D_G$  takes the maximum value  $1/2$  when  $2\alpha^2 \cos^2(r) = 1$ . On the other hand, we know  $\partial E_g/\partial r \geq 0$  for all cases from (37), therefore,  $E_g$  never decrease with the increase of the acceleration parameter  $r$ , but  $E_g$  increase from 0 to its maximum values, then decrease to 0 when  $\alpha^2$  increases from 0 to 1 for a given  $r$ .  $E_g$  has a remarkable character, which different from  $D_g$ , when  $\alpha^2$  varies from 0 to 1.  $E_g$  independent of  $r$ , but  $D_G$  dependent, when  $0 \leq \alpha^2 \leq 1/2$ . This feature is owing to when  $r_{A3} \leq 0, \mathbf{r}_A = -\mathbf{n}$  and  $\mathbf{r}_2 = \mathbf{n}$ ,  $\Lambda_{max}^2 = 1 - \alpha^2$ , then  $E_g = \alpha^2$ . We plot  $D_G$  and  $E_g$  as functions of the acceleration parameter  $r$  for some typical values of  $\alpha^2$  in Fig. 3;  $D_G$  and  $E_g$  as functions of parameter  $\alpha^2$  for some typical values of the acceleration parameter  $r$  in Fig. 4, respectively.

Second, for the special case of  $\alpha = \pm 1/\sqrt{2}$ , our results are different from that of other authors. Alsing et al. investigated the maximally entangled initial state shared by Alice and Rob. They calculated the entanglement of formation, the logarithmic negativity and the mutual information for bipartite subsystems  $\rho_{AI}, \rho_{AII}$  and  $\rho_{III}$  [2]. They also studied the whole tripartite system using the residual tangle (or three tangle). They found the three tangle  $\tau_{A, I, II} = 0$  and concluded that there are no tripartite correlations for any value of the acceleration rate and any entanglements can only exist in the bipartite subsystem. From (18) it is easy to obtain  $D_G(\rho_{AIII}) = \cos^2(r)(1 - \cos^2(r)/2)$ ; using  $E_g = 1 - \Lambda_{max}^2$

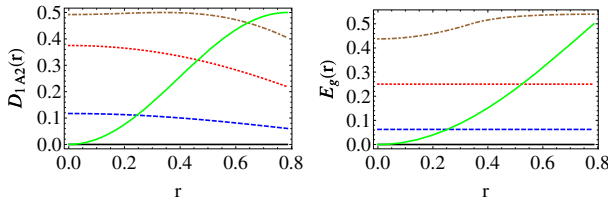


**Fig. 3** (Color online) Plots of geometric measure of quantum discord  $D(\rho_{A|III})$  and geometric measure of entanglement  $E_g(\rho_{A|III})$  as functions of  $r$  for  $|\alpha| = 0$  (thick and black);  $|\alpha| = 0.25$  (dashed and blue);  $|\alpha| = 0.5$  (dotted and red);  $|\alpha| = 0.75$  (dot-dashed and brown);  $|\alpha| = 1.0$  (thick and green)

with (37) we also get  $E_g = 1/2$ , both for  $\alpha = \pm 1/\sqrt{2}$ . These two formulas show even for maximally entangled initial state, the tripartite correlation is always existed. On the other hand, Wang et al. studied a Greeberger-Horne-Zeilinger (GHZ) initially shared by Alice, Bob and Charlie. Then they assume Alice stays stationary while Bob and Charlie move with uniform accelerations. They calculated all  $\pi$ -tangles for bipartite subsystems and the tripartite system. They found when either one or two subsystems of the tripartite state accelerated there is no bipartite entanglement and all the entanglement of this system is in the form of tripartite entanglement. The results of [1] and present paper demonstrate both bipartite and tripartite correlations are existed in the system.

Third, from Section 3, we know  $D_{G(A|III)} \neq D_{G(I|AII)}$ , which is owing to geometric discord only consider a set of local measurements on one subsystem of the whole system, it is not symmetrical for every subsystems of the system. Our results reveal a deeper and essential property: geometric discord is dependent on the observer. This is natural from the view point of relativistic theory. So we can say that the geometric measurements of quantum discord happened to coincide with the theory of relativity on this point.

In summary, we have derived analytical expressions of the geometric discord and the geometric measurement of the entanglement both for the whole Dirac fields in a noninertial system. Our results show an interesting phenomenon that even though two geometric measurements of the total system are not completely coincided with each other in detail, they have similar evolutionary trends with Rob’s acceleration parameter and the entanglement parameter of the initial state. In addition, we showed the geometric discord of Dirac fields in a noninertial system satisfy CKW inequality. It means that Dirac fields in a noninertial system are monogamy for the geometric discord. Furthermore, we revealed that bipartite system and whole tripartite system of the Dirac fields have correlations. Our research is only a small part of this respect. We hope this work could attract much researcher’s attention to study the global quantum properties of various quantum systems in a noninertial system.

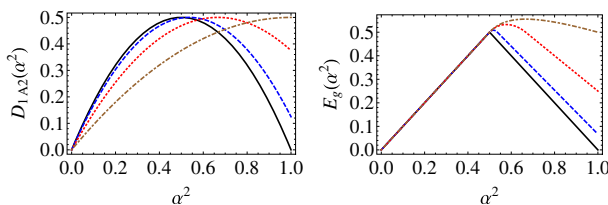


**Fig. 4** (Color online) Plots of geometric measure of quantum discord  $D(\rho_{A|III})$  and geometric measure of entanglement  $E_g(A|III)$  as functions of  $\alpha^2$  for acceleration parameter  $r = 0$  (thick and black);  $r = \pi/12$  (dashed and Blue);  $r = \pi/6$  (dotted and red);  $r = \pi/4$  (dot-dashed and brown)

## References

1. Qiang, W.-C., Zhang, L.: Geometric measure of quantum discord for entanglement of Dirac fields in noninertial frames. *Phys. Lett. B* **742**, 383 (2015)
2. Alsing, P.M. et al.: Entanglement of Dirac fields in non-inertial frames. *Phys. Rev. A* **74**, 032326 (2006)
3. Hwang, M.-R., Park, D., Jung, E.: Tripartite entanglement in a noninertial frame. *Phys. Rev. A* **83**, 012111 (2011)
4. Wang, J., Jing, J.: Multipartite entanglement of fermionic systems in noninertial frames. *Phys. Rev. A* **83**, 022314 (2011)
5. Dakić, B., Vedral, V., Brukner, C.: Necessary and sufficient condition for non-zero quantum discord. *Phys. Rev. Lett.* **105**, 190502 (2010)
6. Luo, S., Fu, S.: Geometric measure of quantum discord. *Phys. Rev. A* **82**, 034302 (2010)
7. Rana, S., Parashar, P.: Tight lower bound on geometric discord of bipartite states. *Phys. Rev. A* **85**, 024102 (2012)
8. Hassan, A.S.M., Lari, B., Joag, P.S.: Tight lower bound to the geometric measure of quantum discord. *Phys. Rev. A* **85**, 024302 (2012)
9. Tufarelli, T. et al.: Quantum resources for hybrid communication via qubit-oscillator states. *Phys. Rev. A* **86**, 052326 (2012)
10. Jung, E. et al.: Reduced state uniquely defines the Groverian measure of the original pure state. *Phys. Rev. A* **77**, 062317 (2008)
11. Tamaryan, L., Park, D.K., Tamaryan, S.: Analytic expressions for geometric measure of three-qubit states. *Phys. Rev. A* **77**, 022325 (2008)
12. Unruh, W.G.: Notes on black-hole evaporation. *Phys. Rev. D* **14**, 870 (1976)
13. Birrel, N.D., Davies, P.C.W.: *Quantum Fields in Curved Space*. Cambridge University, Cambridge (1982)
14. Coffman, V., Kundu, J., Wootters, W.K.: Distributed entanglement. *Phys. Rev. A* **61**, 052306 (2000)